

NAVAL POSTGRADUATE SCHOOL

Monterey, California



6 1515 45

THESIS

SEPARATION IN TIME-DEPENDENT FLOW

by

William H. Butterworth, Jr.

September 1988

Thesis Advisor:

T. Sarpkaya

Approved for public release; distribution is unlimited.

T238719

Unclassified

Security Classification of this page

REPORT DOCUMENTATION PAGE

1a Report Security Classification Unclassified		1b Restrictive Markings	
2a Security Classification Authority		3 Distribution Availability of Report	
2b Declassification/Downgrading Schedule		Approved for public release; distribution is unlimited.	
4 Performing Organization Report Number(s)		5 Monitoring Organization Report Number(s)	
6a Name of Performing Organization Naval Postgraduate School		7a Name of Monitoring Organization Naval Postgraduate School	
6b Office Symbol (If Applicable) 69		7b Address (city, state, and ZIP code) Monterey, CA 93943-5000	
6c Address (city, state, and ZIP code) Monterey, CA 93943-5000		9 Procurement Instrument Identification Number	
8a Name of Funding/Sponsoring Organization		8b Office Symbol (If Applicable)	
8c Address (city, state, and ZIP code)		10 Source of Funding Numbers	
		Program Element Number	Project No
		Task No	Work Unit Accession No
11 Title (Include Security Classification) Separation in Time-Dependent Flow			
12 Personal Author(s) William H. Butterworth, Jr.			
13a Type of Report Master's Thesis		13b Time Covered From To	14 Date of Report (year, month, day) 1988 September
15 Page Count 44			
16 Supplementary Notation The views expressed in this thesis are those of the author and do not reflect the official policy or position of the Department of Defense or the U.S. Government.			
17 Cosati Codes		18 Subject Terms (continue on reverse if necessary and identify by block number)	
Field	Group	Subgroup	
19 Abstract (continue on reverse if necessary and identify by block number)			
The angular motion of separation points on a smooth cylinder immersed in a sinusoidally oscillating flow has been determined experimentally through the use of a U-shaped water tunnel, a special differential pressure probe, and a data acquisition system. The results have been compared with those obtained previously by Grass and Kemp for a single amplitude of oscillation through the use of flow visualization. The results have shown that the separation points undergo large angular excursions during a given cycle, the degree of excursion depending on the Reynolds number and the Keulegan-Carpenter number. The separation data obtained in this exploratory investigation will form the basis of future numerical analysis of oscillating flow about cylinders.			
20 Distribution/Availability of Abstract		21 Abstract Security Classification	
<input checked="" type="checkbox"/> unclassified/unlimited <input type="checkbox"/> same as report <input type="checkbox"/> DTIC users		Unclassified	
22a Name of Responsible Individual Professor T. Sarpkaya		22b Telephone (Include Area code) (408) 646-3425	22c Office Symbol 69S1

DD FORM 1473, 84 MAR

83 APR edition may be used until exhausted

security classification of this page

All other editions are obsolete

Unclassified

Approved for public release; distribution is unlimited.

Separation in Time-Dependent Flow

by

William H. Butterworth, Jr.
Lieutenant, United States Navy
B.M.E., Villanova University, 1979

Submitted in partial fulfillment of the
requirements for the degree of

MASTER OF SCIENCE IN MECHANICAL ENGINEERING
and
MECHANICAL ENGINEER

from the

NAVAL POSTGRADUATE SCHOOL
September 1988

ABSTRACT

The angular motion of separation points on a smooth cylinder immersed in a sinusoidally oscillating flow has been determined experimentally through the use of a U-shaped water tunnel, a special differential pressure probe, and a data acquisition system. The results have been compared with those obtained previously by Grass and Kemp for a single amplitude of oscillation through the use of flow visualization. The results have shown that the separation points undergo large angular excursions during a given cycle, the degree of excursion depending on the Reynolds number and the Keulegan-Carpenter number. The separation data obtained in this exploratory investigation will form the basis of future numerical analysis of oscillating flow about cylinders.

TABLE OF CONTENTS

I. INTRODUCTION.....	1
II. EXPERIMENTAL EQUIPMENT AND PROCEDURES.....	7
A U-SHAPED WATER TUNNEL.....	7
B TEST CYLINDER.....	7
III. PRESENTATION AND DISCUSSION OF RESULTS.....	11
A THE CASE OF $K = 8$	11
B THE CASE OF $K = 20$	13
C THE CASE OF $K = 40$	14
IV. CONCLUSIONS.....	18
APPENDIX FIGURES.....	20
LIST OF REFERENCES.....	33
INITIAL DISTRIBUTION LIST.....	35

LIST OF FIGURES

1	Front View of U-Shaped Water Tunnel	20
2	Interior of the U-Shaped Water Tunnel.....	21
3	Sample Trace of Flow Acceleration and Differential Pressure ($K = 8$, $\phi = 0$ degrees)	22
4	Sample Trace of Flow Acceleration and Differential Pressure ($K = 40$, $\phi = 160$ degrees)	23
5	Variation of Instantaneous Velocity and Direction of Ambient Flow	24
6a	Instantaneous Position of Separation Point at the Upper Half of the Cylinder for $K = 8$	25
6b	Instantaneous Position of Separation Point at the Lower Half of the Cylinder for $K = 8$	26
7a	Instantaneous Position of Separation Point at the Upper Half of the Cylinder for $K = 20$	27
7b	Instantaneous Position of Separation Point at the Lower Half of the Cylinder for $K = 20$	28
7c	Instantaneous Position of Separation Points at Upper and Lower Halves of the Cylinder for $K = 20$	29
8a	Replot of Grass and Kemp Flow Visualization Data for $K = 38$	30
8b	Instantaneous Position of Separation Point at the Upper Half of the Cylinder for $K = 40$	31
8c	Instantaneous Position of Separation Point at the Lower Half of the Cylinder for $K = 40$	32

TABLE OF SYMBOLS AND ABBREVIATIONS

A	Amplitude at the test section
D	Cylinder diameter
K	Keulegan-Carpenter number $K = U_m T / D$
Re	Reynolds number $Re = U_m D / \nu$
T	Period of oscillation
t	Time
U_m	Maximum velocity
u	Instantaneous velocity
θ_s	Separation angle measured counter-clockwise from positive x-direction
ν	Kinematic viscosity
ϕ	Position of wire probe measured positive clockwise from vertical

ACKNOWLEDGMENTS

The author takes this opportunity to express his gratitude to Distinguished Professor T. Sarpkaya for sharing his knowledge and wisdom over the course of this investigation. His understanding of life, people, nature, and, of course, hydrodynamics made this a well-balanced and most enjoyable learning experience. I thank you, Professor.

Thanks also to Mr. Jack McKay for his technical expertise and cheerful nature during the experimentation.

Special recognition is due my wife and children. To Marion, for her unending love, support, and confidence in me, and to the boys, for always brightening my day and helping me to put things in the proper perspective. I love you all.

I. INTRODUCTION

The separated steady and unsteady flows about bluff bodies have been almost completely unyielding to both analysis and numerical simulation for a number of mathematical reasons and fundamental fluid dynamic phenomena. Separation gives rise to the formation of free shear layers which roll up into vortex rings or counter-rotating vortices. They, in turn, interact with each other, with the counter-sign vorticity generated at the base of the body, and with the motion of often unknown separation points. The wake becomes unsteady even for a steady ambient flow and the problem of the determination of the characteristics of the wake becomes coupled to the conditions prevailing upstream of the separation points. Evidently, viscosity modifies radically the inviscid flow, which, in this case, cannot serve even as a first approximation to the actual flow. The boundary layer equations are not applicable beyond the separation points and are, therefore, of limited use in bluff-body flow problems. Fage and Johansen's pioneering experimental work (1928), Gerrard's (1966) vortex formation model, and Roshko's (1954) numerous contributions, followed by a large number of important papers, have provided extremely useful insights into the mechanism of vortex shedding. It became clear that a two-dimensional body immersed in a two-dimensional steady flow does not give rise to a two-dimensional steady wake and only a fraction (about 60 percent for a circular cylinder) of the original circulation

survives the vortex formation. It also became clear that bluff-body flows exhibiting separation, turbulence, and time dependence are almost completely unyielding to both analysis and simulation, even if the ambient flow is assumed to be time invariant. Many flows of practical interest are unsteady, i.e., the characteristics of the ambient flow are time dependent.

In the past 20 years or so, a large number of theoretical and experimental studies have been carried out. These dealt primarily with unseparated laminar flows, the early stages of impulsively started flow over plates and cylinders (numerical and experimental studies), and oscillating flows with zero or non-zero mean flow (on an infinite flat plate and over a cylinder with streaming flow, all under laminar flow conditions) for the purpose of studying the effects of flow unsteadiness on the transition mechanism and turbulence development (see, e.g., Bradbury, et al., 1982). Very little has been attempted, either theoretically or experimentally, to analyze the wake-boundary-layer interaction in time-dependent flows (i.e., with unsteady ambient flow). The subject of separated time-dependent flow at large Reynolds numbers is lesser developed but of greater practical importance (particularly to marine-related topics) relative to other classical component disciplines of fluid mechanics.

A number of unsteady flow machines and their use in the investigation of unsteady turbulent boundary layers have been reviewed and documented by Carr (1981). These included flat plate, diffuser, pipe, airfoil, and cascade flows. The results have shown that (1) the time-

averaged mean velocity profile is almost always the same as the velocity profile that would occur in a steady flow having an equivalent mean external flow velocity; (2) the turbulent structure in the oscillating flow is not changed from the equivalent steady-state counterpart; and (3) the unsteady effects are often confined to a thin layer near the wall, while the outer region of the boundary layer is not strongly affected. These conclusions, apparently valid for unsteady turbulent boundary layer flows, are not applicable to unsteady separated, turbulent, bluff-body flows. The separated unsteady flow situations involving wake return, as in the case of a sinusoidally oscillating flow about a cylinder, or wake retardation, as in the case of a decelerating parachute, are an order of magnitude more complex. In steady flow, the position of the separation points is nearly stationary, except for small excursions of about three degrees (on a circular cylinder). Furthermore, the interference between the vortices and the body is confined mostly to the vortex formation region. For oscillating flows, the net effect of the shed vortices is twofold. Firstly, their return to the body dramatically affects the boundary layer, outer flow, pressure distribution, and the generation and survival rate of the new vorticity. Secondly, they not only give rise to additional separation points (during the early stages of the flow reversal) but also strongly affect the motion of the primary separation points. These effects are further compounded by the diffusion and decay of vortices and by the three-dimensional nature of the flow (all of which give rise to cycle-to-cycle variations, numerous flow modes, etc.). The stronger and better

correlated the returning vortices, the sharper and more pronounced the changes are in the pressure distribution on the body and in the integrated quantities such as lift, drag, and inertia coefficients. Nevertheless, the increased correlation does not entirely eliminate the consequences of the stochastic variations in the motion of vortices.

In periodic flow, the mobile separation points (when they are not fixed by sharp edges) undergo large excursions (as much as 120 degrees during a given cycle of oscillating flow over a circular cylinder). This experimental fact renders the treatment of boundary layers on bluff bodies subjected to periodic wake return extremely difficult, particularly when the state of the boundary layer changes during a given cycle. Furthermore, the classical criterion of separation for steady flow, i.e., the vanishing of skin friction on the body, is no longer valid for unsteady flow. According to the MRS criterion (Moore, 1958; Rott, 1956; and Sears, 1972), it is the simultaneous vanishing of the shear and velocity at a point within the boundary layer that determines the separation point. It is clear from the foregoing that there is little hope of devising a satisfactory theoretical model before something is understood of the unsteady processes associated with the formation and reversal of the wake, spanwise coherence, and the sensitive dependence of the motion of vortices on small changes in the previous conditions and on the nature of transition in oscillating flow about smooth and rough cylinders.

For steady ambient flow about bluff bodies, the numerical studies based on the use of the steady or unsteady form of the Navier-Stokes

equations and some suitable spatial and temporal differencing schemes are limited, out of necessity, to relatively low Reynolds numbers (less than about 1,000) (see, e.g., Lecointe and Piquet, 1984, for a finite difference solution and Gresho, et al., 1984, for a finite element solution). The major obstacles to the application of either the finite difference or the finite element methods to higher Reynolds number laminar flow are stability, computation time, treatment of the boundary conditions, and accuracy. Even though many differencing schemes have been developed to overcome the instability problem (Roache, 1972), maintaining stability continues to be a problem with increasing Reynolds number. The truncation errors decrease the apparent Reynolds number by introducing an unknown artificial viscosity. Even if the problems associated with stability and truncation errors were to be resolved, the attempt to obtain solutions of the Navier-Stokes equations at higher Reynolds numbers are limited by a fundamental fluid dynamic phenomenon: the stability of the flow itself. When the flow becomes turbulent either in the wake and/or in the boundary layers, one needs a closure model for turbulence to solve the Reynolds equations for a time-dependent, three-dimensional, separated, turbulent flow (even if the ambient flow is smooth and the bluff body is two-dimensional). Clearly, the roots of the most serious problem in the solution of the Navier-Stokes equations are buried in the physics of turbulence. The stability and truncation-error problems associated with the differencing schemes may be resolved but the problem of turbulence appears to transcend all efforts.

The numerical solution of unsteady incompressible Navier-Stokes equations in their vorticity-stream-function formulation has been investigated by numerous researchers through the use of various finite-difference techniques. These studies concern mostly the separated flow about circular cylinder and prisms at relatively low Reynolds numbers (see, e.g., Davis and Moore, 1982).

It appears that the existing numerical methods cannot yet treat the high Reynolds number flows with sufficient accuracy for a number of reasons. The finite difference schemes require a very fine grid, a turbulence model, and a very large computer memory. It seems that the modeling of the turbulent stresses in the wake, particularly in time-dependent flows, will be the major source of difficulty in all future calculations. Whether it will ever be practical to apply the finite difference and finite element methods to high Reynolds number flows is unknown. The inherent difficulties are certainly significant enough to warrant exploring other solution methods.

The present investigation is an exploratory experimental study of the motion of separation points on a smooth circular cylinder immersed in a sinusoidally oscillating flow. The results are expected to form the basis of all numerical studies in providing guidance for their formulation as well as comparison for their accuracy and validity.

II. EXPERIMENTAL EQUIPMENT AND PROCEDURES

A U-SHAPED WATER TUNNEL

The U-shaped water tunnel, used in the present investigation, has been described in detail in numerous theses (see, e.g., O'Keefe, 1986). Here only a brief description, together with the modifications made to it for its adaptation to the present investigation, is presented. The water tunnel consists of a three feet by five feet by 30 feet horizontal section and two vertical legs of three feet by six feet by 17 feet (see Figures 1 and 2).

The top of one of the legs of the tunnel is connected to an air supply system. A butterfly valve near the top of the tunnel oscillates with a frequency exactly equal to that of the natural frequency of the water in the tunnel. The flow amplitude may be maintained at the desired level and as long as desired by adjusting a gate in front of the fan supplying the air.

The instantaneous acceleration and hence the displacement of water is measured by means of a differential pressure transducer, connected to the pressure taps shown in Figure 2 and analyzed subsequently together with signals coming from other transducers.

B TEST CYLINDER

A single, smooth, 5.460-inch aluminum cylinder was used in the experiments. It spanned the entire test section and there were no gaps between the cylinder ends and the tunnel walls. At two

diametrically opposed points on a section of the cylinder pressure taps for the measurement of differential pressure between two points, separated by a small wire, were drilled. Each pressure tap was 1/64 inch diameter and the center-to-center distance was 0.020 inches. The wire had a diameter of 0.006 inches and a length of 0.15 inches. The axis of the wire was normal to the direction of flow. Initially, it was planned to have two hot film skin-friction probes mounted in the same cross-section but at the ends of a diameter normal to that joining the pressure taps. The unfortunate leakage of water into the electrical wires of the hot film probes eliminated their further use.

Each of the differential pressure taps was connected to a pressure transducer, carefully drained to remove air and electronically balanced through the use of a carrier amplifier and recorder system. One of the pressure transducers had a capacity of ± 100 inches of water and the other ± 300 inches of water. Preliminary experiments with both transducers have shown that the use of the higher-capacity transducer will not provide stable enough signals to measure the small differential pressure across the wire probe. This was particularly made clear from the evaluation of the preliminary data that the sign change in the differential pressure and the precise time at which it occurred are of prime importance. Evidently, the success of the technique depended on the fact that when the separation point coincides with the particular position of the wire probe, then, and at that instant, the differential pressure across the wire is zero. At all other times, the flow over the wire (in either direction) yields a differential pressure, signifying that

the separation is not at the position of the wire and that it must either be fore or aft of the wire. It is clear that the purpose of the very existence of the wire is to cause a larger differential pressure than that which would normally occur between the two extremely close pressure taps. It is also clear that the wire had to be as small as it is to prevent it from behaving like a surface roughness on an otherwise smooth cylinder. As will be seen later, the wire probe has served the intended purpose well.

The procedure for the performance of the experiments was as follows. The tunnel was filled to the desired level, the dissolved air was allowed to escape (often overnight), the electronic system was warmed up for about an hour, the transducers were nulled, and the signals were connected to an analog recorder and to a high-speed data acquisition system, capable of acquiring digitized data at a rate of 100,000 samples/second. The entire system was monitored and the data analyzed with a desk-top computer.

Figures 3 and 4 show sample traces of flow acceleration and differential pressure measured across the wire probe as a function of normalized time. These figures show the times at which the differential pressure has changed its sign, i.e., the times at which the flow reversed itself at the particular position of the wire probe. The data were obtained in this manner at suitable angles relative to the horizontal axis by rotating the cylinder axis (from outside the tunnel) at suitable intervals. The experiments were carried out for four *Keulegan-Carpenter* numbers, defined by

$$K = 2\pi \frac{A}{D} = \frac{U_m T}{D} \quad (1)$$

in which A is the amplitude of the flow oscillation at the test section, D is the diameter of the cylinder, U_m is the maximum velocity in the cycle, and T is the period of the flow oscillation. The four nominal values of K were 8, 13.5, 20, and 40. Here, however, only the data obtained with $K = 8$, 20, and 40 are reported. The case of $K = 13.5$ needs the acquisition of additional data for the tracking of the motion of the separation points which will be reported at a later date.

III. PRESENTATION AND DISCUSSION OF RESULTS

The data are presented for the three cases separately. In each case, the motion of the separation point is tracked on the upper and lower halves of the cylinder as a function of time. Furthermore, the motion of the separation points is shown schematically on an inset depicting the cylinder and the critical times in the cyclic history of the separation points.

Figure 5 shows the variation of the instantaneous velocity $u = U_m \cos(2\pi t/T)$ together with the instantaneous direction of the flow relative to the positive x -direction. Clearly, the flow is in the negative x -direction in the interval $0 \leq t/T \leq 0.25$ and decelerating; the flow is in the positive x -direction in the interval $0.25 \leq t/T \leq 0.75$ and accelerating in the interval $0.25 \leq t/T \leq 0.50$ and decelerating in the interval $0.50 \leq t/T \leq 0.75$; and finally, again the flow is in the negative x -direction in the interval $0.75 \leq t/T \leq 1.0$ and accelerating toward its maximum value. The significance of the directions and rates of change of the magnitude of velocity will become apparent in connection with the interpretation of the motion of the separation points.

A THE CASE OF $K = 8$

Figures 6a and 6b show the instantaneous position of the separation points at the upper and lower halves of the cylinder, respectively, as a function of the normalized time t/T .

As the flow decelerates in the negative x -direction, the separation point at the top half of the cylinder moves rapidly from about $\theta_s = 90$ degrees (measured counter-clockwise from the positive x -axis) to about $\theta_s = 40$ degrees as the ambient flow comes to a momentary rest. The motion of the separation points during a short interval, preceding and following the $u = 0$ instant, is dictated primarily by the residual motion of the fluid and of the remaining shed vortices. Considering the fact that the velocities induced on the cylinder and the differential pressure across the wire probe are extremely small and the fact that there may not be one or more clearly definable separation points, the acquisition of meaningful separation data becomes nearly impossible. A short time later, however, ($t/T \approx 0.4$), and as the flow accelerates in the x -direction the separation point, which must have been lingering at $\theta_s = 40$ degrees becomes clearly identifiable and moves toward the top shoulder of the cylinder ($\theta_s = 90$ degrees) as the flow reaches its maximum velocity and then decelerates to zero at $t/T = 0.75$. During the later parts of the deceleration period, the separation point quickly moves toward $\theta_s \approx 140$ degrees. Following a brief period during which there is no clearly identifiable separation point, the flow begins to accelerate rapidly in the negative x -direction and the separation point once again begins to move from $\theta_s = 140$ degrees toward $\theta_s = 90$ degrees. The foregoing description of the separation point is shown in a schematic way on the inset, where the corresponding letters and arrows identify the limits and the direction of motion of the separation points.

Figure 6b shows the motion of the separation point at the lower half of the cylinder. As in the case of the top half, the separation angle oscillates between $\theta_s \approx -40$ degrees and $\theta_s \approx -140$ degrees. Furthermore, a comparison of the motions of the separation points on the upper and lower halves of the cylinder shows that they are more or less mirror images of each other (with an extremely small phase shift of about $\Delta(t/T) = 0.015$). This shows that at such small Keulegan-Carpenter numbers the flow behaves as if it started impulsively and symmetrically at each half cycle. Before closing the discussion of the case of $K = 8$, one has to note that the acquisition of additional data, both at smaller increments of cylinder rotation and with more wire probes, will be essential in delineating the instantaneous positions of the separation points more precisely.

B. THE CASE OF $K = 20$

Figures 7a and 7b show the motion of the separation points at the top and bottom halves of the cylinder. At the top half, θ_s begins at about 135 degrees when the flow is at its maximum value in the negative x-direction. Subsequently, it moves toward the shoulder of the cylinder and stays at approximately 75 degrees, as one would normally expect the separation to occur in steady flow had the velocity remained at a constant value of U_m . When the flow reverses its direction at $t/T = 0.75$, the separation point jumps to about $\theta_s = 145$ degrees and then decreases to about 135 to 140 degrees, returning the flow conditions on the top half of the cylinder to the starting conditions.

Similar observations are made regarding the motion of the separation points at the bottom half of the cylinder, as seen from a comparison of Figures 7a and 7b, and more clearly in Figure 7c. The last figure also shows that the separation points are not symmetrically situated at the corresponding times, as in the case of $K = 8$. This is entirely expected and the reason for it is due to the asymmetric shedding of vortices on either side of the cylinder. Additional details of the respective position of the separation points may be deduced from the circular plot in the inset.

C. THE CASE OF $K = 40$

This particular Keulegan-Carpenter number was chosen for two reasons. One was to track the separation points at sufficiently high K values and the other was to obtain data at a K value for which there is some other data for comparison. Grass and Kemp (1979), using a 1.97-inch cylinder, aluminum particles, and a camera, determined rather crudely (± 10 degrees) the angular position of the separation points on smooth and roughened cylinders for $K = 38$. Their data are reproduced here from a replot of the original data by Sarpkaya and Isaacson (1981) (see Figure 8a). According to Grass and Kemp, the separation point oscillates between about 50 and 150 degrees. These data are compared later with that obtained in the present investigation.

Figures 8b and 8c show the position of the separation points at the top and bottom halves of the cylinder, respectively. Shortly after $t/T = 0.75$, i.e., after the start of the flow to accelerate in the negative x -direction, the separation angle starts at a relatively large angle ($\theta_s =$

140 degrees). This is expected on the grounds that the flow at each cycle starts as if it started anew impulsively from rest and that the separation for such a flow is normally at $\theta = 180$ degrees. However, because of the background turbulence remaining from the previous cycles of oscillation, the separation at the start of the cycle is a little smaller and, as noted above, at $\theta_s = 110$ degrees, as seen in Figure 8b either at $t/T = 0$ or at $t/T = 1.0$. As the flow begins to decelerate while moving in the negative x-direction, θ_s moves toward the top of the cylinder and reaches a minimum value of $\theta_s \approx 70$ degrees, and more or less remains there throughout the acceleration and deceleration period of the flow in the positive x-direction. Shortly before the ambient flow comes to a complete stop, θ_s increases very rapidly from 90 to about 140 degrees, completing one cycle of the flow and of the angular motion of the separation point at the top half of the cylinder.

Figure 8c shows the angular motion of the separation point at the bottom half of the cylinder. A careful examination of this figure and comparison of it with Figure 8b show that the separation point at the bottom half of the cylinder follows nearly exactly the same path, with the following exception. The events that occur at the first quadrant of the circle at a given time t_1/T occur at the third quadrant at $t/T = t_1/T + 0.5$. Considering the fact that the data were independently obtained for the top and bottom halves, the said correspondence is rather remarkable. The matching of the motion of the separation point with a phase difference of 0.5 is equally satisfactory as far as the second and fourth quadrants are concerned.

Now one is in a position to compare Figure 8b with that obtained by Grass and Kemp, even though the latter is highly subjective. The general trend of the two sets of data for smooth cylinders is about the same for the motion of flow starting from rest and eventually coming to rest during a given half cycle, θ_s starts at a fairly high value, decreases to about 70 degrees, and then restarts at the beginning of a new half cycle. There are, however, major differences between Figures 8a and 8b as far as the actual values and the rates of change of θ_s are concerned. For example, Grass and Kemp data shows that θ_s drops to values as low as 50 degrees. The present data shows a minimum of 70 degrees. Furthermore, near the end of the deceleration and the beginning of a new half cycle, Grass and Kemp data shows no dramatic change in the position of θ_s whereas, according to the present data, the separation point moves rather quickly from about 90 degrees to about 140 degrees. Moreover, there is no indication in Grass and Kemp data as to what happens at the lower half of the cylinder and how the motion of the separation points on the two halves of the cylinder interact with each other. It is now clear that, as the vortices are shed alternately and asymmetrically on one or the other side of the cylinder, one should not expect a synchronized motion between the two separation points as in the case of $K = 8$. Lastly, not all the differences between the present data and that of Grass and Kemp can or should be attributed to the subjective nature of the latter. It is worth noting that the highest Reynolds number in the Grass and Kemp experiments is about 54,200 and in the present experiments is about

130,000. It is a well-known fact that the drag coefficient decreases rapidly with increasing Reynolds number for a given K (Sarpkaya and Isaacson, 1981). In fact, for $K = 40$, the minimum drag coefficient appears at a Reynolds number of $Re = U_m D/\nu \approx 150,000$. It is also a well-known fact that, at least in steady flow, the smaller the drag, the smaller the size of the wake, and vice versa. The two sets of data compared here are in conformity with that fact and tend to partly explain the values at the two extremes of the separation point excursion.

IV. CONCLUSIONS

The results presented herein warranted the following conclusions. First, it is shown that the separation points can be accurately determined through the use of a wire probe and differential pressure across it. This method surely eliminates all the ambiguities associated with the flow visualization techniques.

Second, it is shown that at a Keulegan-Carpenter number of eight and, presumably, lower values, the angular motion of the separation points at the top and bottom halves of the cylinder are nearly symmetrical. This shows that the flow behaves as if it started impulsively anew at each half cycle and that the vortices generated grow and shed symmetrically.

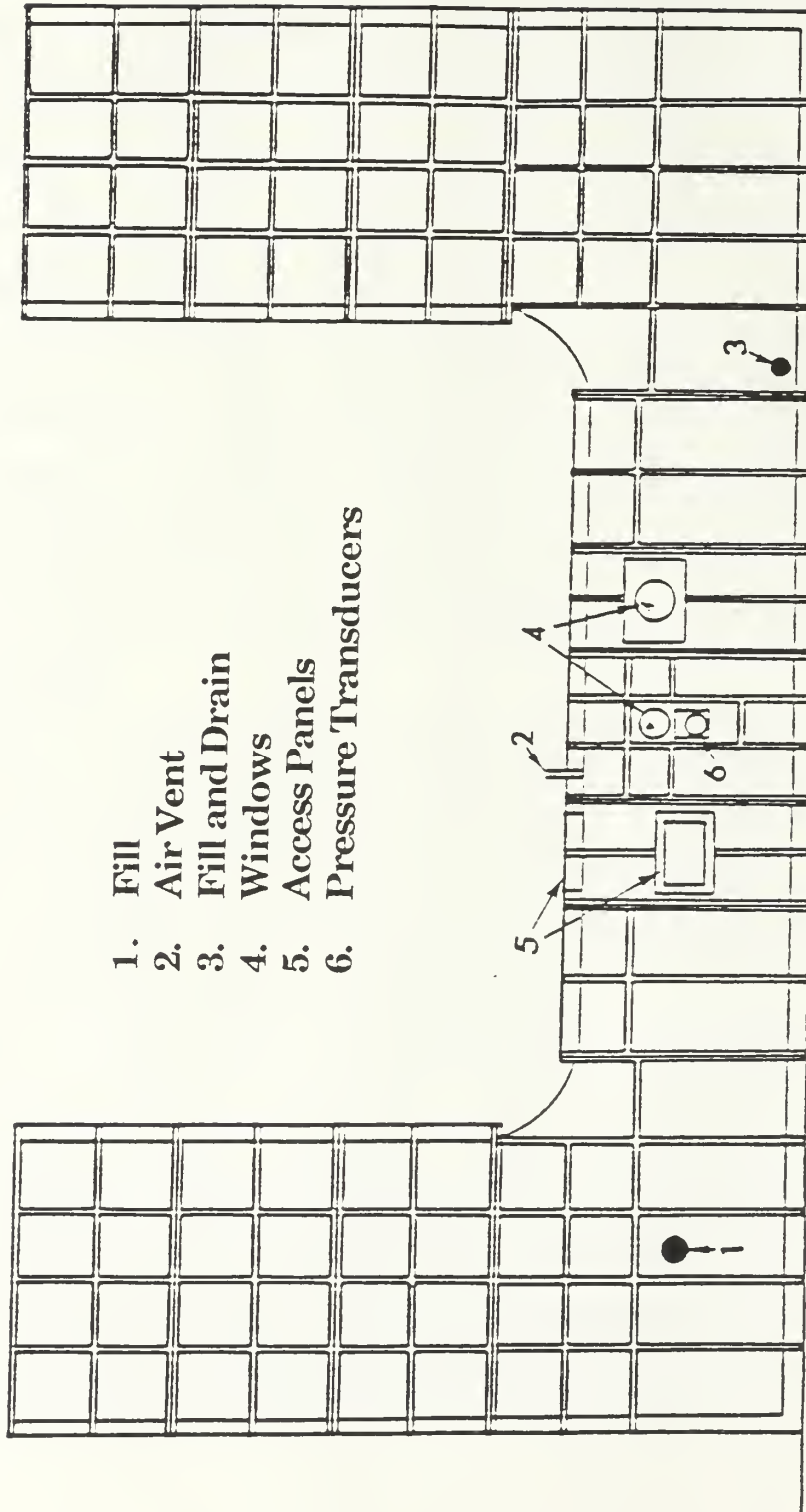
Third, it is shown that at larger Keulegan-Carpenter numbers, such as $K = 20$ and $K = 40$, the excursion of the separation points on top and bottom of the cylinder is not symmetrical. However, the events occurring on the top half of the cylinder at a given time do occur one-half cycle later at the bottom half.

Last, the separation point data presented herein, as unique and reliable as they are, are expected to form the basis for comparison of all numerical models attempting to predict the behavior of sinusoidally oscillating flow about a cylinder. Such a comparison will serve as a better test of the accuracy of the numerical methods than the comparison of the integrated quantities such as lift and drag forces. It is because of

this reason that the present investigation is being pursued with larger number and variety of wire probes, with other smooth and rough cylinders, and at other Keulegan-Carpenter numbers.

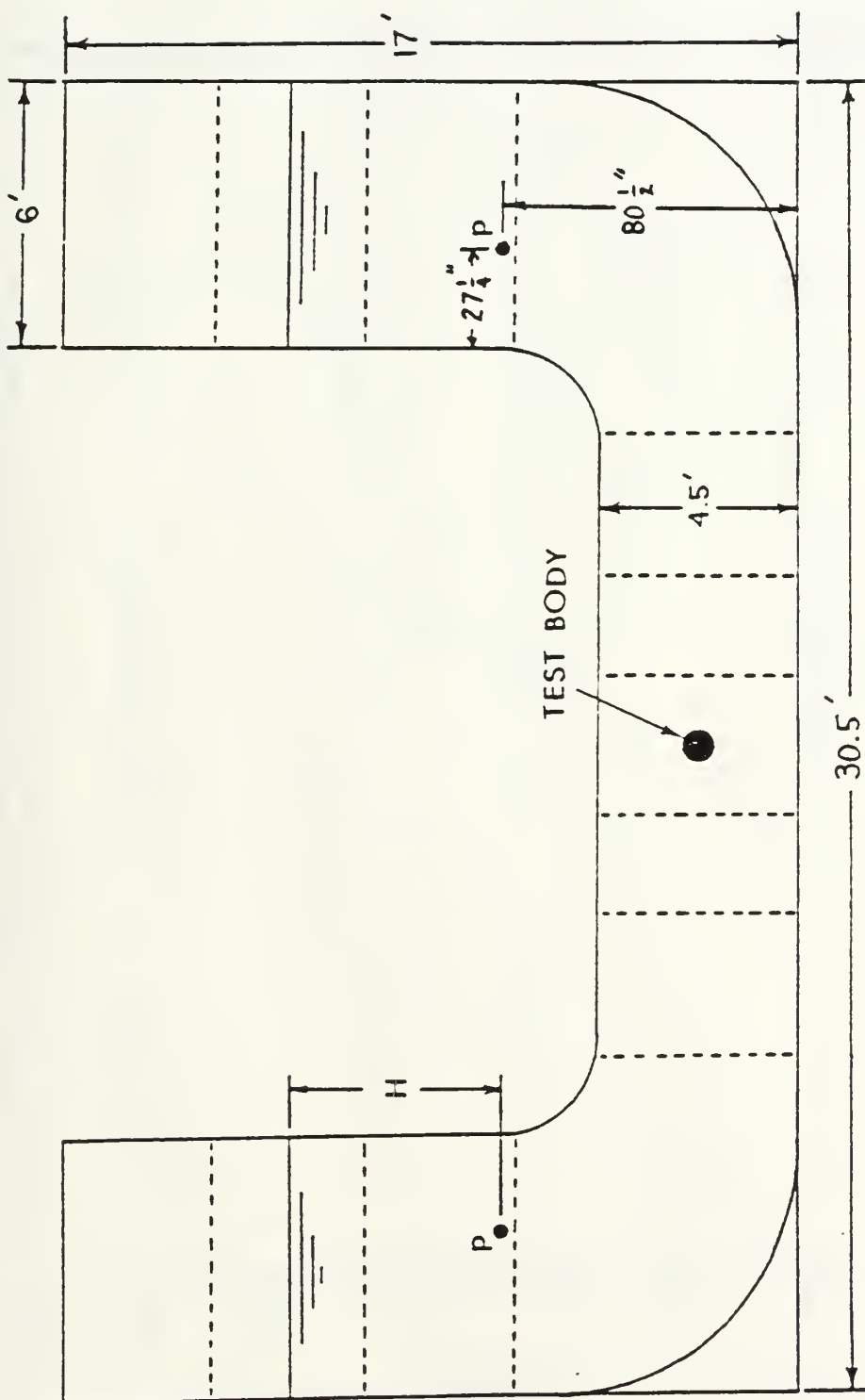
APPENDIX

FIGURES

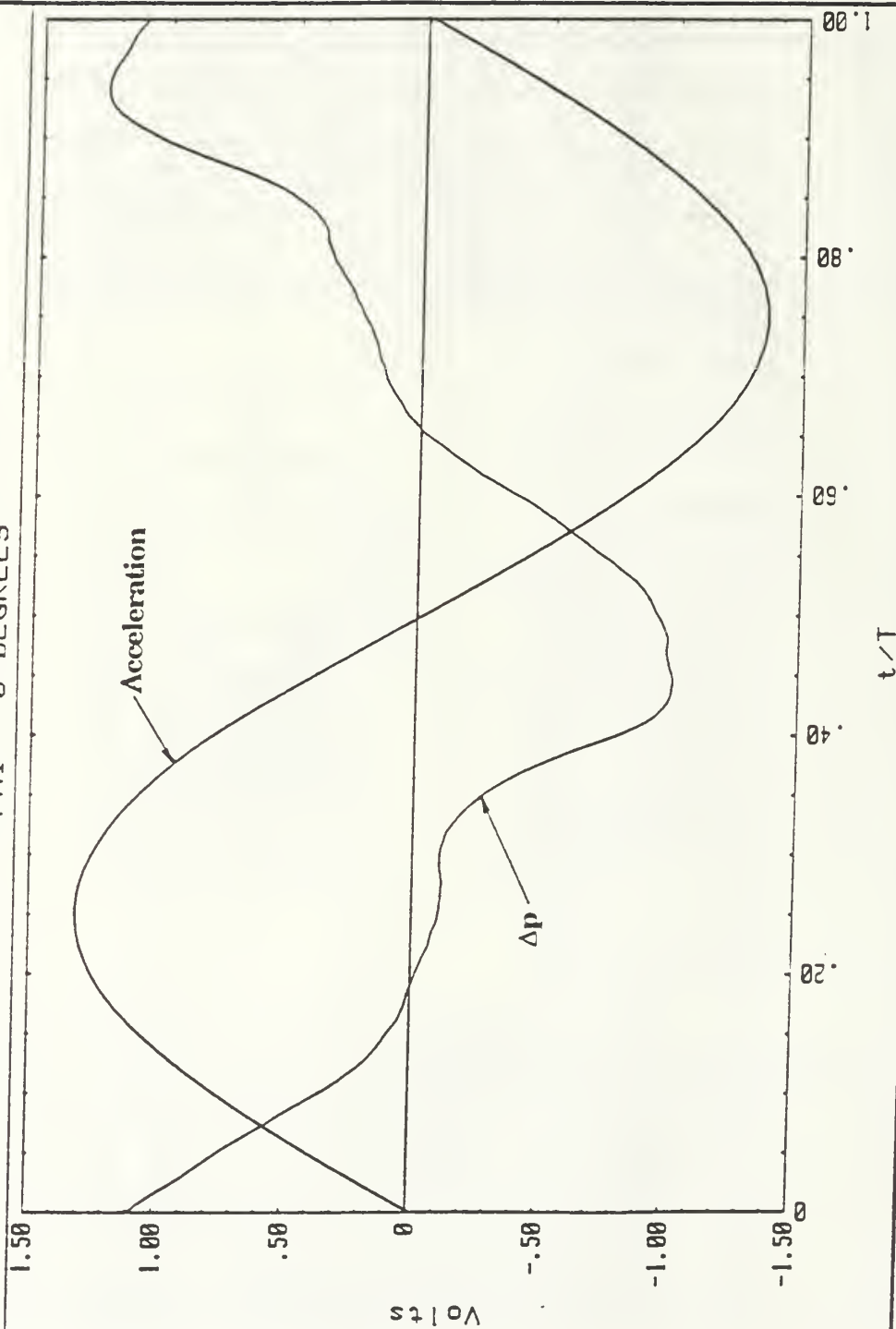


1. Fill
2. Air Vent
3. Fill and Drain
4. Windows
5. Access Panels
6. Pressure Transducers

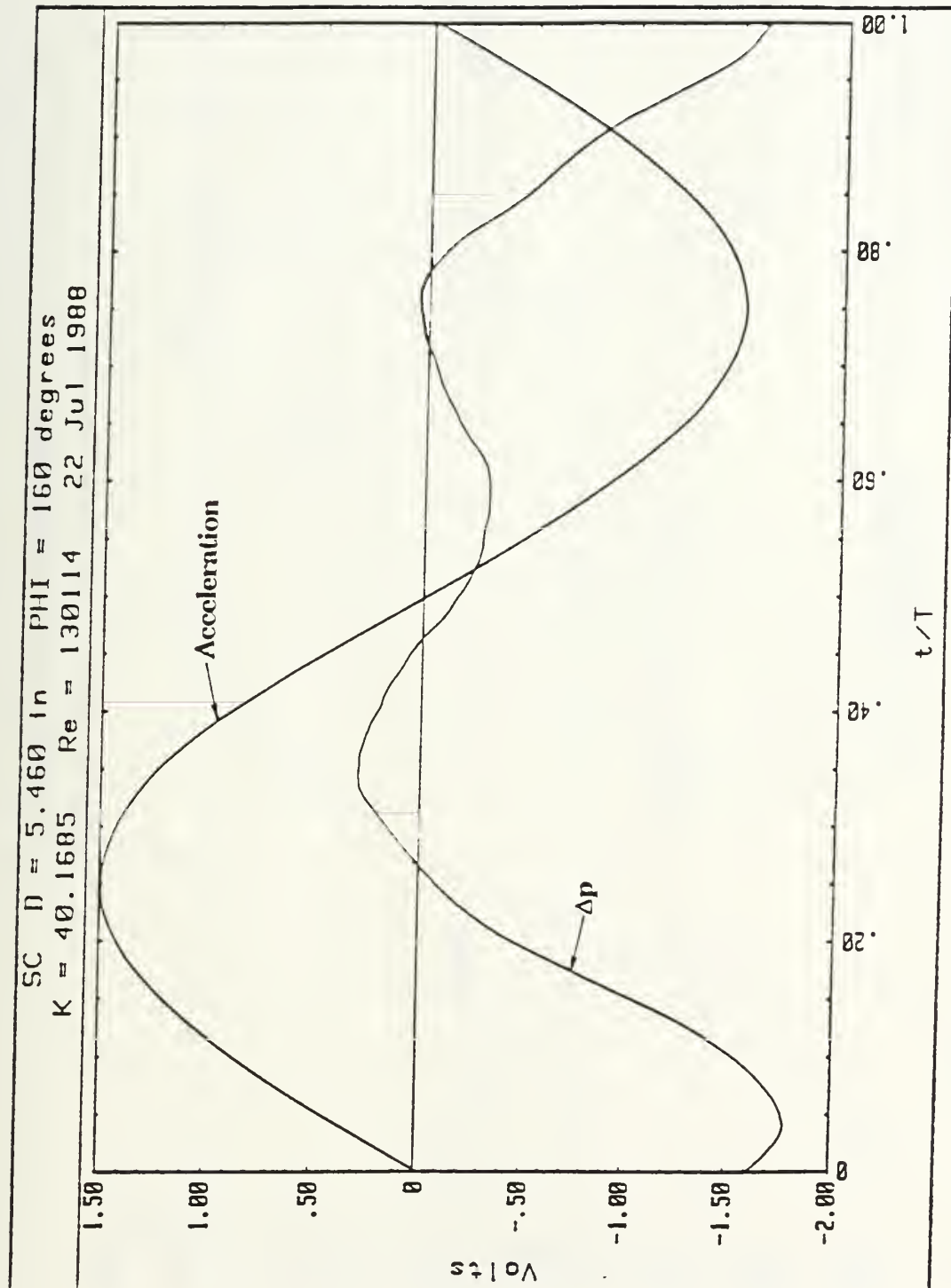
1. Front View of U-Shaped Water Tunnel



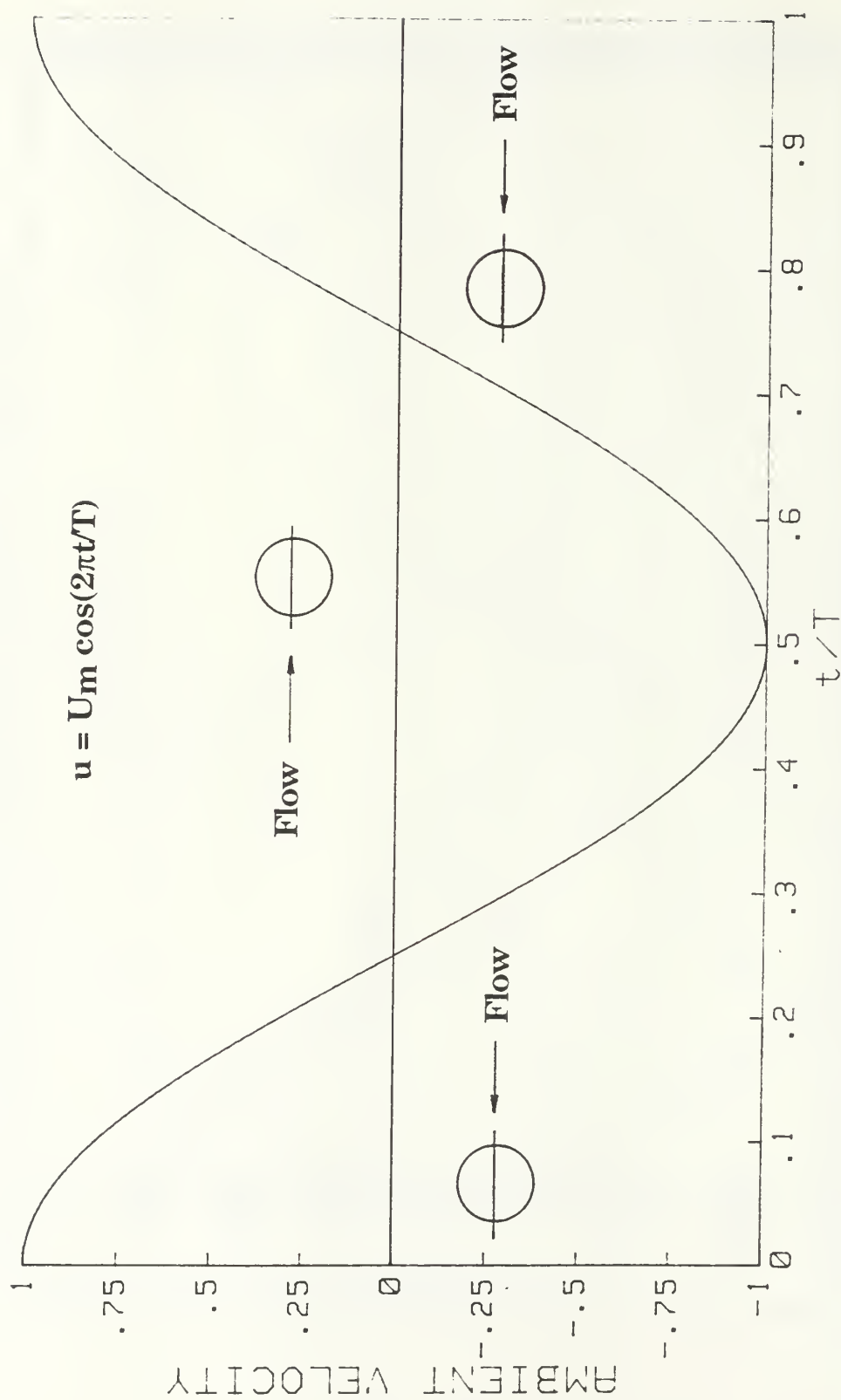
K = 7.21 SC D = 5.460 in 08 JUL 88
 PHI = 0 DEGREES



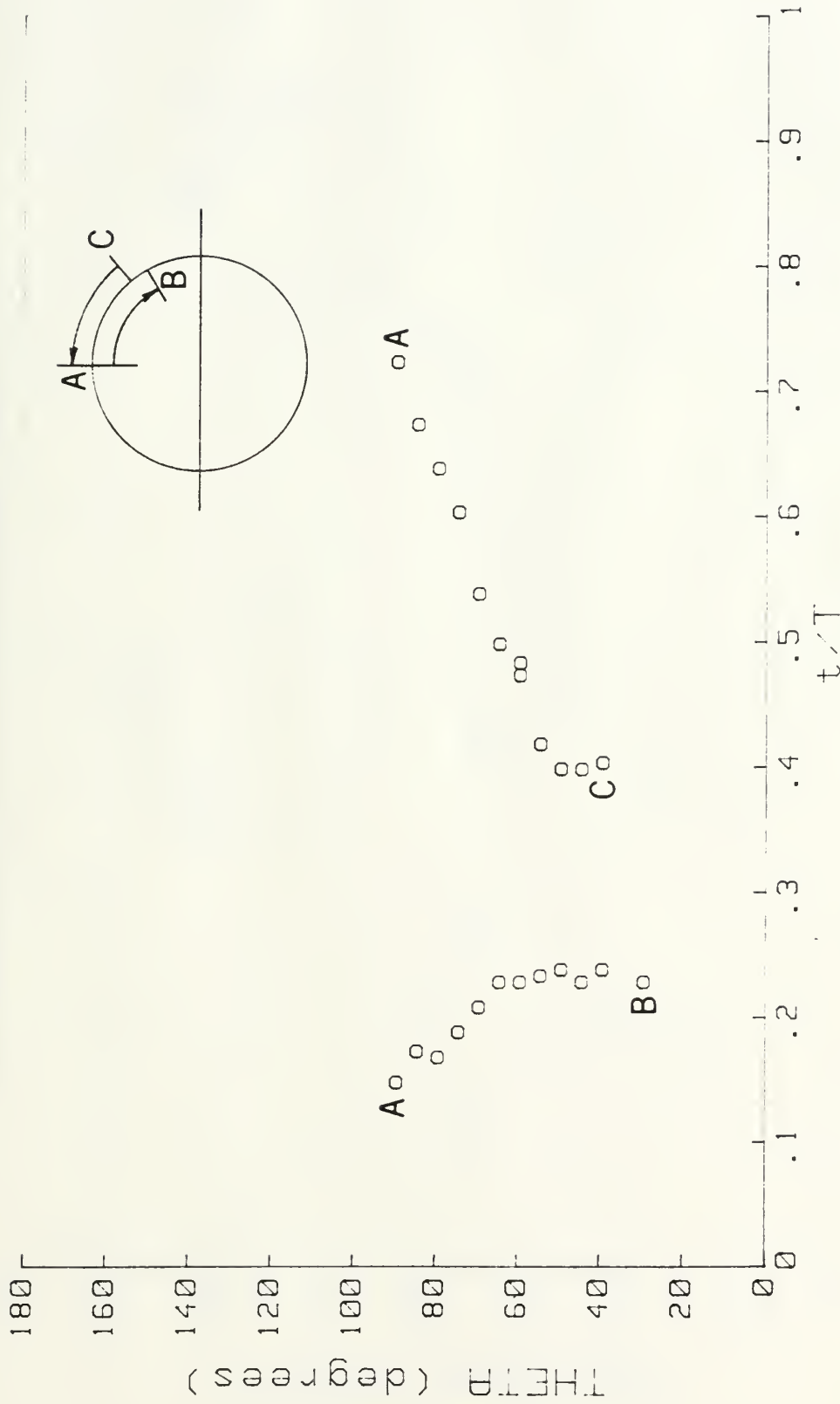
3. Sample Trace of Flow Acceleration and Differential Pressure ($K = 8$, $\phi = 0$ degrees)



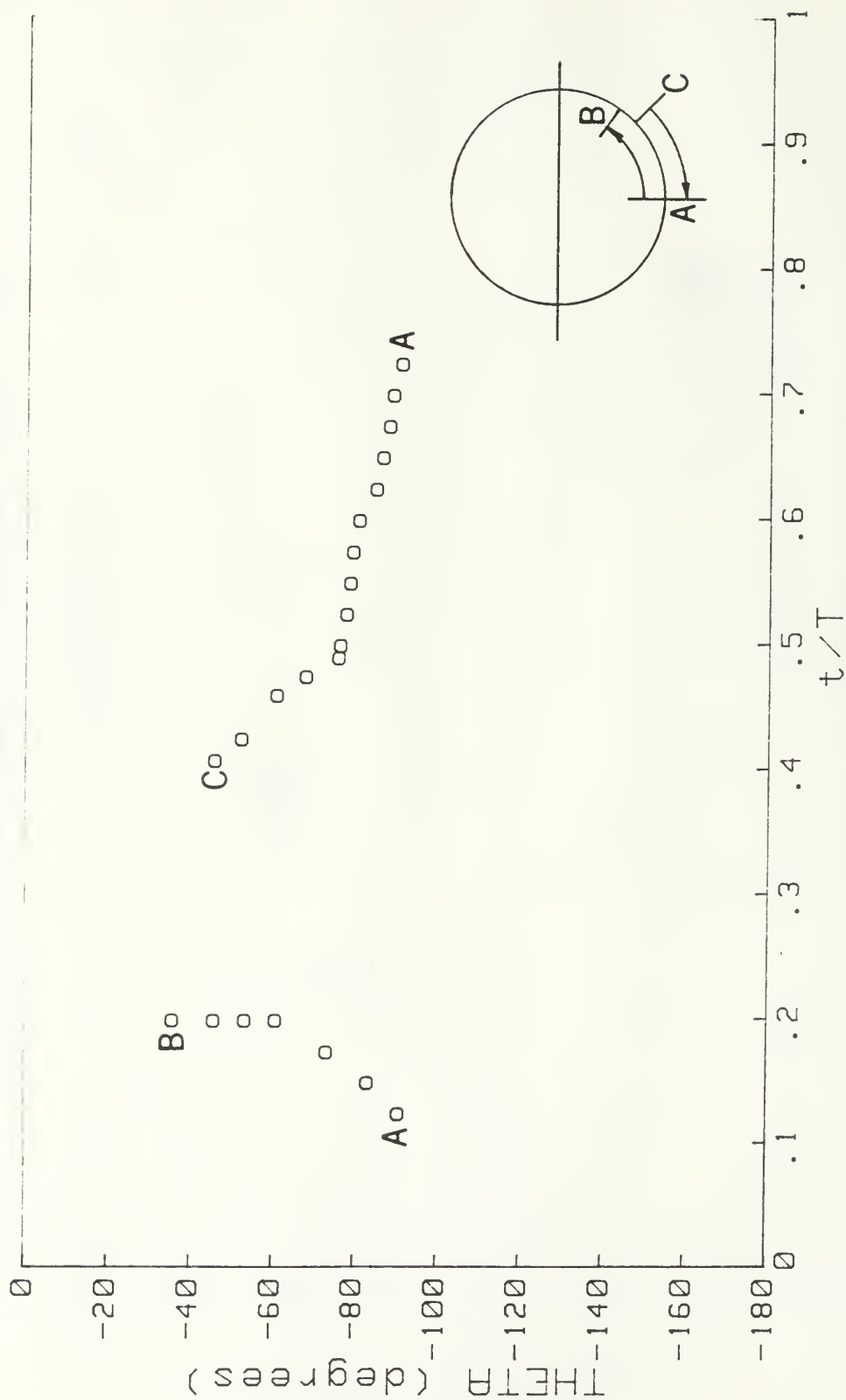
4. Sample Trace of Flow Acceleration and Differential Pressure ($K = 40$, $\phi = 160$ degrees)



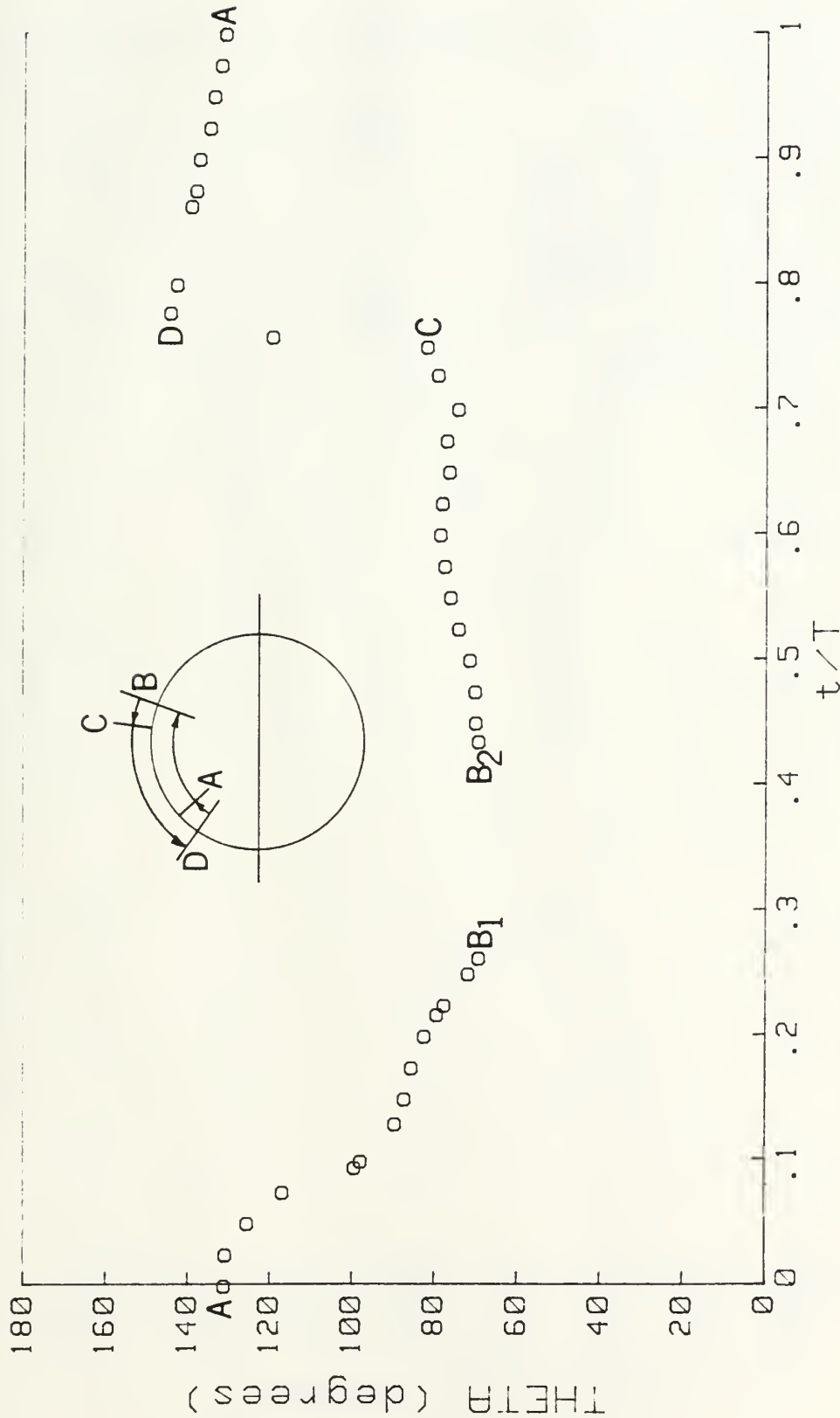
5. Variation of Instantaneous Velocity
and Direction of Ambient Flow



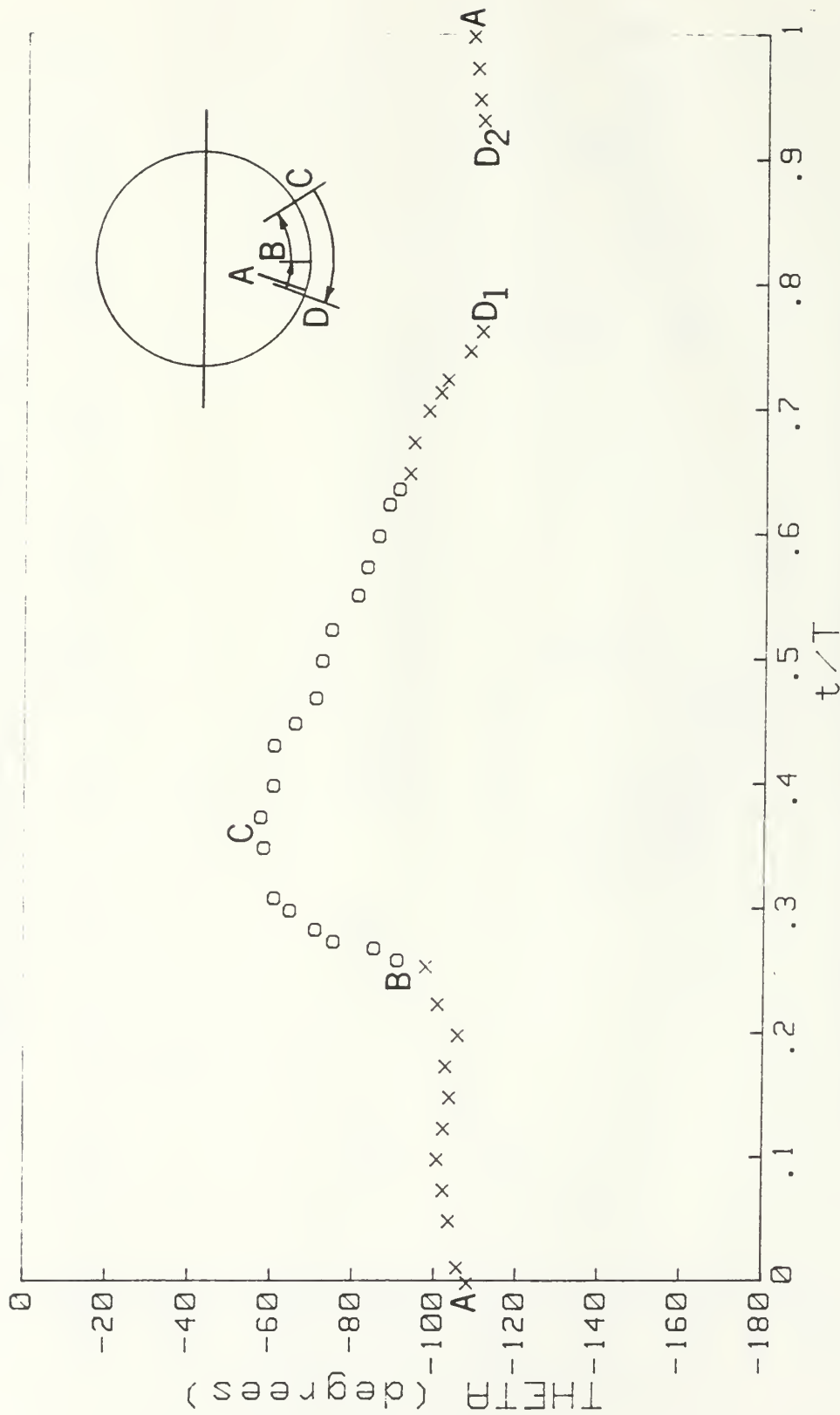
6a. Instantaneous Position of Separation Point at the
Upper Half of the Cylinder for $K = 8$



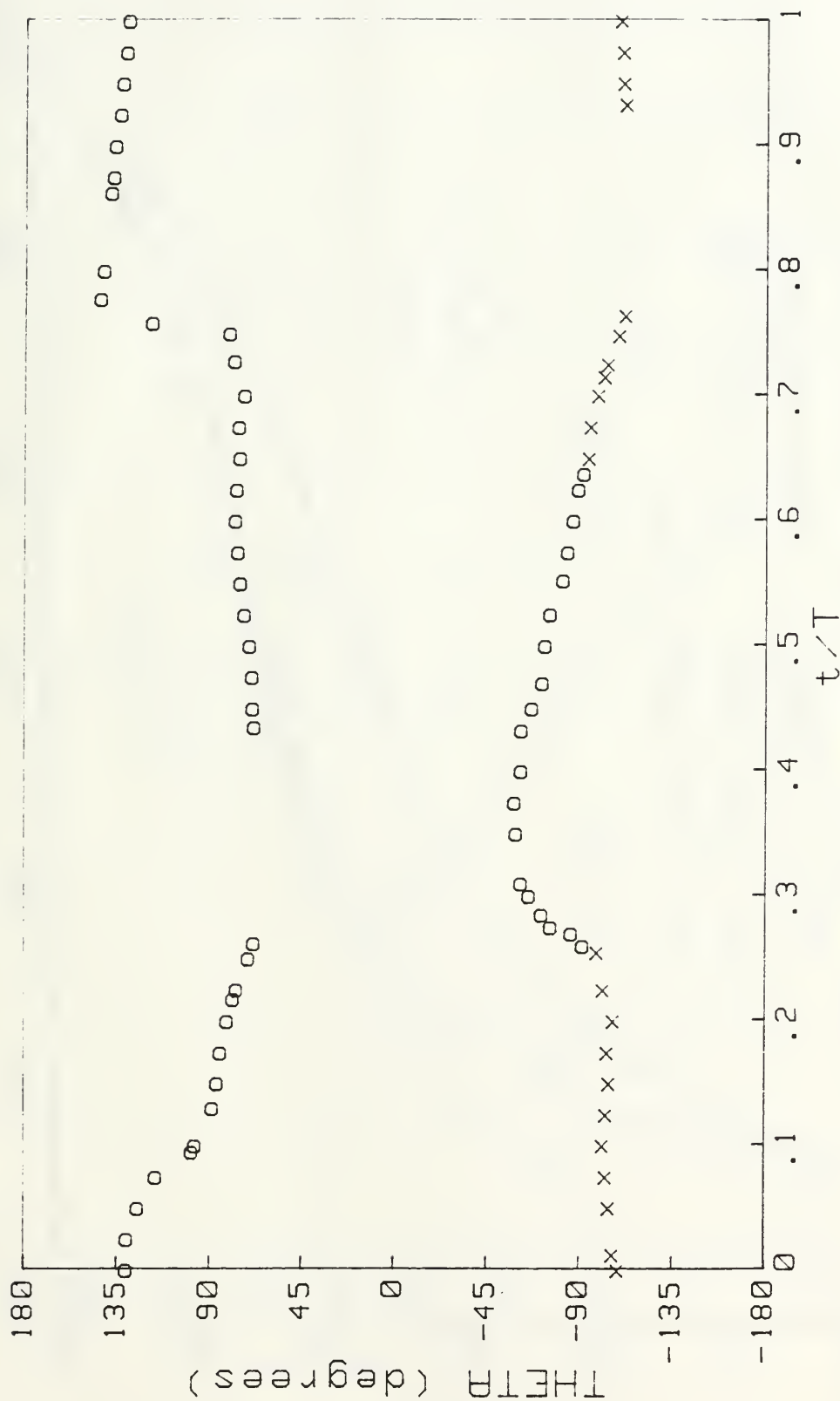
6b. Instantaneous Position of Separation Point at the Lower Half of the Cylinder for $K = 8$



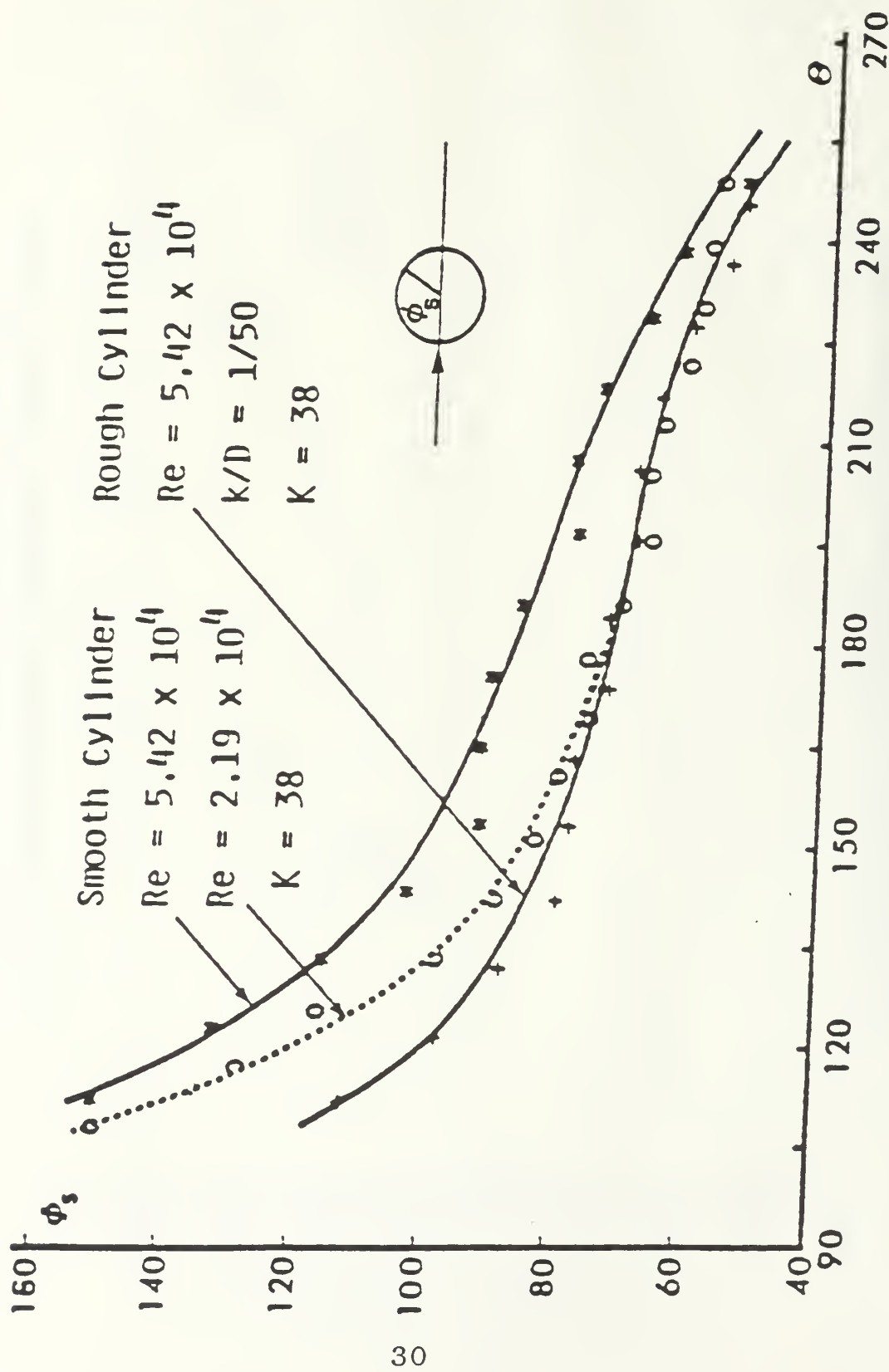
7a. Instantaneous Position of Separation Point at the
Upper Half of the Cylinder for $K = 20$



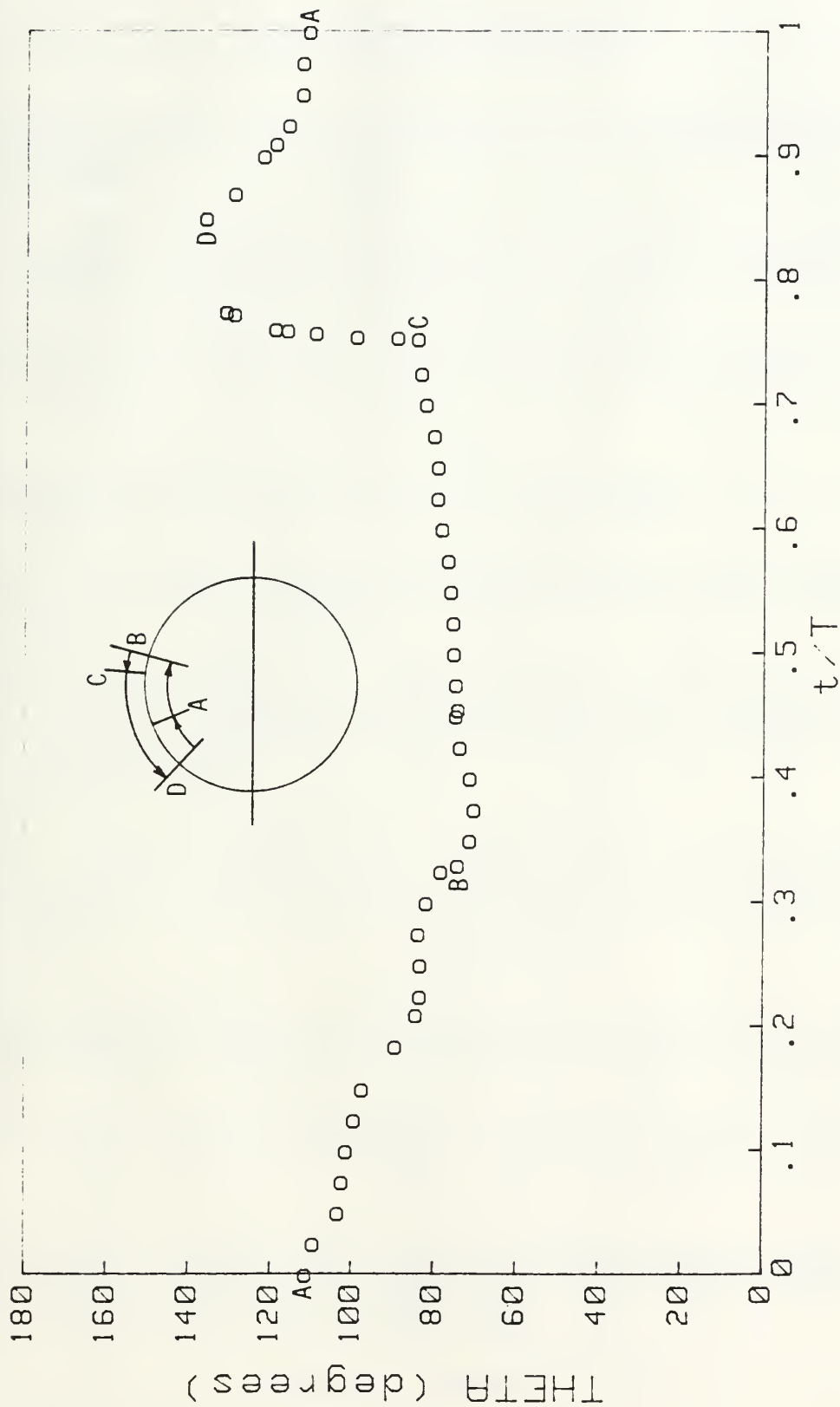
7b. Instantaneous Position of Separation Point at the
Lower Half of the Cylinder for $K = 20$



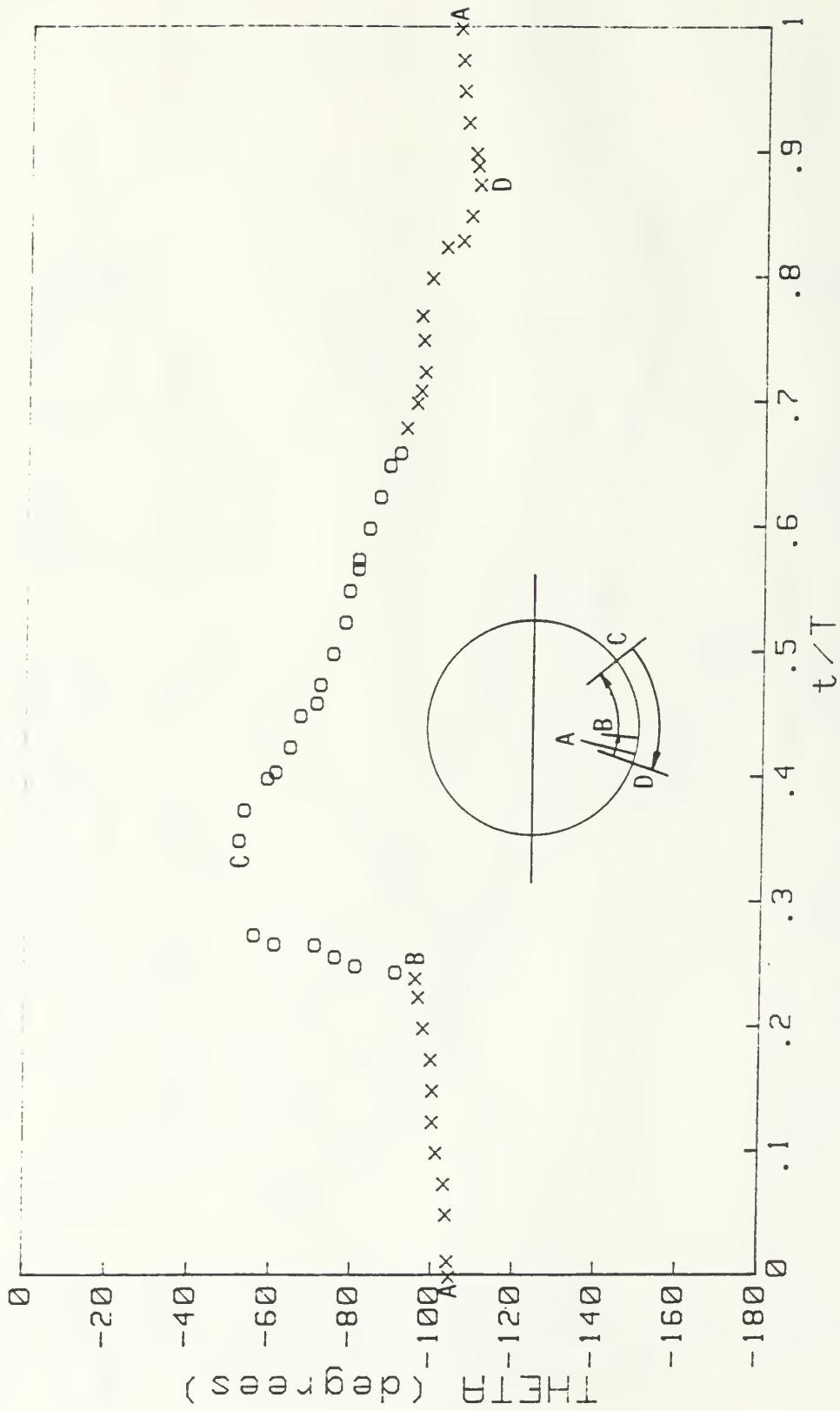
7c. Instantaneous Position of Separation Points at Upper
and Lower Halves of the Cylinder for $K = 20$



8a. Replot of Grass and Kemp Flow Visualization Data for $K = 38$



8b. Instantaneous Position of Separation Point at the
Upper Half of the Cylinder for $K = 40$



8c. Instantaneous Position of Separation Point at the
Lower Half of the Cylinder for $K = 40$

LIST OF REFERENCES

Bradbury, L. J. S., Durst, F., Launder, B. E., Schmidt, F. W., and Whitelaw, J. H. (eds.), *Turbulent Shear Flows-III*, New York: Springer-Verlag, 1982.

Carr, L. W., "A Review of Unsteady Turbulent Boundary-Layer Experiments," in *Unsteady Turbulent Shear Flows*, R. Michael, et al., eds., New York: Springer-Verlag, 1981, pp. 3-34.

Davis, R. W., and Moore, E. F., "A Numerical Study of Vortex Shedding from Rectangles," *Journal of Fluid Mechanics*, v. 116 (1982), pp. 475-506.

Fage, A., and Johansen, R. C., "The Structure of Vortex Sheets," *Aeronautical Research Council R&M*, n. 1143 (1928).

Gerrard, J. H., "The Mechanics of the Formation Region of Vortices Behind Bluff Bodies," *Journal of Fluid Mechanics*, v. 25 (1966), pp. 401-413.

Grass, A. J., and Kemp, P. H., "Flow Visualization Studies of Oscillatory Flow Past Smooth and Rough Circular Cylinders," in *Mechanics of Wave-Induced Forces on Cylinders*, T. L. Shaw, ed., London: Pitman, 1979, pp. 406-420.

Gresho, P. M., Chan, S. T., Lee, R. L., and Upson, C. D., "A Modified Finite Element Method for Solving the Time Dependent, Incompressible Navier-Stokes Equations, Part 2: Applications," *International Journal of Numerical Methods in Fluids*, v. 4 (1984), pp. 619-640.

Lecointe, Y., and Piquet, J., "On the Use of Several Compact Methods for the Study of Unsteady Incompressible Viscous Flow Round a Circular Cylinder," *Computers in Fluids*, v. 12 (1984), pp. 255-280.

Moore, F. K., "On the Separation of Unsteady Laminar Boundary Layer," UTAM Symposium, Boundary Layers, Freiberg, 1958, pp. 296-311.

O'Keefe, J. L., *Time-Dependent Flow About Bilge Keels and Smooth and Rough Circular Cylinders*, M.S. and M.E. Thesis, Naval Postgraduate School, Monterey, California, March 1986.

Roache, P. J., "On Artificial Viscosity," *Journal of Computational Physics*, v. 10 (1972), pp. 169-184.

Roshko, A., "On the Drag and Shedding Frequency of Two-Dimensional Bluff Bodies," *NACA Technical Note* no. 3169, 1954.

Rott, N., "Unsteady Viscous Flow in the Vicinity of a Stagnation Point," *Quarterly Applied Mathematics*, v. 13 (1956), pp. 444-451.

Sarpkaya, T., and Isaacson, M., *Mechanics of Wave Forces on Offshore Structures*, New York: Van Nostrand Reinhold Company, 1981.

Sears, W. R., "Unsteady Motion of Airfoils with Boundary-Layer Separation," *AIAA Journal*, v. 14 (1972), pp. 216-220.

INITIAL DISTRIBUTION LIST

	<u>No. Copies</u>
1. Defense Technical Information Center Cameron Station Alexandria, VA 22304-6145	2
2. Library, Code 0142 Naval Postgraduate School Monterey, CA 93943-5002	2
3. Department Chairman, Code 69 Department of Mechanical Engineering Naval Postgraduate School Monterey, CA 93943-5000	2
4. Professor T. Sarpkaya, Code 69Sl Department of Mechanical Engineering Naval Postgraduate School Monterey, CA 93943-5000	10
5. Commanding Officer David Taylor R & D Center Carderrock Laboratory Bethesda, MD 20084	1
6. Naval Sea Systems Command PMS 350 Washington, DC 20362	1
7. LT William H. Butterworth, Jr. 4026 Bleigh Avenue Philadelphia, PA 19136	2

Thesis
B951545 Butterworth
c.1 Separation in time-de-
pendent flow.

Thesis
B951545 Butterworth
c.1 Separation in time-de-
pendent flow.

UERGCU



thesB951545

Separation in time-dependent flow.



3 2768 000 84918 6

DUDLEY KNOX LIBRARY